18th International Conference on Structural Mechanics in Reactor Technology (SMiRT 18)
Beijing, China, August 7-12, 2005
SMiRT18-J11-5

THREE-DIMENSIONAL DYNAMIC SOLUTION OF LAMINATED SHELL PANEL WITH PIEZOELECTRIC SENSOR LAYER BASED ON THE THEORY OF ELASTICITY

Ali Reza Daneshmehr *
Scientific Board Member, Islamic Azad Univ. (IAU), central Tehran Branch, Mech. Eng. Dep., 424, Hafez Ave., 15875-4413, Tehran 14838-17173, Tehran/ Iran
Phone: +98-21-3790661, Fax: +98-21-6419736
E-mail: alidaneshmehr@yahoo.com

Mahmoud Shakeri
Professor, Dept. of Mechanical Engineering, Amirkabir univ. of Tech., Tehran / Iran
E-mail: shakeri@cic.aut.ac.ir

ABSTRACT

Elasticity solution is presented for finitely long, simply supported, orthotropic, piezoelectric shell panel under dynamic pressure excitation. Only the direct effect of piezoelectric is considered. The highly coupled partial differential equations (p.d.e.) are reduced to ordinary differential equations (o.d.e.) with variable coefficients by means of trigonometric function expansion in circumferential and axial directions. The resulting ordinary differential equations are solved by Galerkin finite element method. Numerical examples are presented for [0/90/P] lamination. Finally the results are compared with the published results.

Keywords: piezoelectric, panel, elasticity, three-dimensional, sensor

1. INTRODUCTION

The development of a new class of smart composite materials and adaptive structures with sensory/active capabilities may further improve the performance and reliability of aeronautical structural systems. Such materials will combine the superior mechanical properties of composite materials, as well as incorporated the additional inherent capability to sense and adapt their static and dynamic response (adaptive structures), or continuously monitor the type, location, and extent of eminent damage (health monitoring).

Therefore, the integration of piezoelectric materials and structural composites has become the subject of focus in the area of smart materials and structures and numerous papers on this subject have been published.

Tzou and his co-workers published a series of papers on finite element and analytical analysis of piezoelectric shell-type continua (e.g., Tzou and Gadre, 1989; Tzou, 1992; Tzou and Tseng, 1991; Tzou et al., 1994).Using Hamilton's principle and linear piezoelectricity, Tzou derived the system equations for piezoelectric shell vibrations (Tzou and Zhong, 1993, 1994). In addition to approximate analysis, exact studies of piezoelectric circular cylindrical shells (Chen et al., 1996) and infinite panel (Dumir et al., 1997) were also performed. Kapuria and his co-workers presented three-dimensional solution for axisymetric cylindrical shell (Kapuria et al. 1997). The authors obtained elasticity solution of orthotropic thick laminated cylindrical panels subjected to dynamic loading (2003). Authors presented analysis of thick laminated panel with piezoelectric actuators and sensors based on three-dimensional theory of elasticity, too (2003, 2004). Finally; the response analysis of the infinite piezoelectric shell panel actuators based on the theory of elasticity was also performed by author (2004).

In this paper, the dynamic elastic solution of cross-ply laminated panel with piezoelectric sensor layer is presented. The panel is subjected to pressure excitation and three dimensional elasticity solution is used.

The shell panel is simply supported at four sides. The highly coupled partial differential equations (p.d.e.) are reduced to ordinary differential equations (o.d.e.) with variable coefficients by means of trigonometric function expansion in circumferential and axial directions. The resulting ordinary differential equations are solved by Galerkin finite element method. Finally three layered panels with a piezoelectric layer under dynamic load are solved and the results are compared with latest published results.

2. BASIC EQUATIONS AND BOUNDARY CONDITIONS

The equations of motion in the absence of body force in cylindrical coordinates are

$$\sigma_{r,r} + \frac{\sigma_r - \sigma_\theta}{r} + \frac{1}{r}\tau_{r\theta,\theta} + \tau_{zr,z} = \rho\frac{\partial^2 u_r}{\partial t^2}$$

$$\tau_{r\theta,r} + \frac{1}{r}\sigma_{\theta,\theta} + \tau_{z\theta,z} + 2\frac{\tau_{r\theta}}{r} = \rho\frac{\partial^2 u_\theta}{\partial t^2} \qquad \text{(Eq. 1)}$$

$$\tau_{rz,r} + \frac{\tau_{z\theta,\theta}}{r} + \sigma_{z,z} + \frac{1}{r}\tau_{rz} = \rho\frac{\partial^2 u_z}{\partial t^2}$$

The charge equation of equilibrium of electrostatics in cylindrical coordinates is (Tzou 1994)

$$D_{r,r} + \frac{D_r}{r} + \frac{D_{\theta,\theta}}{r} + D_{z,z} = 0 \qquad \text{(Eq. 2)}$$

The strain-displacement relations and the electric-potential (ψ) relations of the piezoelectric medium are written as (Dumir 1997)

$$\varepsilon_{ij} = \frac{1}{2}(u_{i,j} + u_{j,i}) \qquad \text{(Eq. 3)}$$

$$E_i = -\psi_{,i} \qquad \text{(Eq. 4)}$$

The linear constitutive equations of a piezoelectric medium are given by

$$\sigma = C\varepsilon - e^T E \qquad D = e\varepsilon + \eta E \tag{Eq. 5}$$

where the superscript T denotes the transpose of a matrix. The components of stress σ, strain ε, electric field E and electric displacement D are given in cylindrical coordinate system (r,θ,z), by

$$\sigma = [\sigma_r \quad \sigma_\theta \quad \sigma_z \quad \tau_{\theta z} \quad \tau_{rz} \quad \tau_{r\theta}]^T, \quad E = [E_r \quad E_\theta \quad E_z]^T,$$

$$\varepsilon = [\varepsilon_r \quad \varepsilon_\theta \quad \varepsilon_z \quad \gamma_{\theta z} \quad \gamma_{rz} \quad \gamma_{r\theta}]^T,$$

$$D = [D_r \quad D_\theta \quad D_z]^T, \quad C = \begin{bmatrix} C_{11} & C_{12} & C_{13} & 0 & 0 & 0 \\ C_{12} & C_{22} & C_{23} & 0 & 0 & 0 \\ C_{13} & C_{23} & C_{33} & 0 & 0 & 0 \\ 0 & 0 & 0 & C_{44} & 0 & 0 \\ 0 & 0 & 0 & 0 & C_{55} & 0 \\ 0 & 0 & 0 & 0 & 0 & C_{66} \end{bmatrix}, \quad e = \begin{bmatrix} e_{33} & e_{31} & e_{32} & 0 & 0 & 0 \\ 0 & 0 & 0 & 0 & 0 & e_{15} \\ 0 & 0 & 0 & 0 & e_{24} & 0 \end{bmatrix},$$

$$\eta = \begin{bmatrix} \eta_1 & 0 & 0 \\ 0 & \eta_2 & 0 \\ 0 & 0 & \eta_3 \end{bmatrix}$$

C_{ij} , e_{ij} and η_{ij} denote, respectively, the components of the matrices of elastic, piezoelectric and dielectric constants of the piezoelectric materials.

After substitution Eqs.(3-6) into Eqs.(1) and (2), the governing equations of equilibrium in terms of displacements for each layer of cylindrical panel are obtained.

$$\begin{aligned}
&\left[c_{11}\frac{\partial^2}{\partial r^2} + \frac{c_{11}}{r}\frac{\partial}{\partial r} - \left(\frac{c_{22}}{r^2} - \frac{c_{66}}{r^2}\frac{\partial^2}{\partial\theta^2} - c_{55}\frac{\partial^2}{\partial z^2}\right)\right]u_r + \left[\frac{c_{12}+c_{66}}{r}\frac{\partial^2}{\partial r\partial\theta} - \frac{c_{22}+c_{66}}{r^2}\frac{\partial}{\partial\theta}\right]u_\theta \\
&+\left[(c_{13}+c_{55})\frac{\partial^2}{\partial r\partial z} - \frac{c_{23}-c_{13}}{r}\frac{\partial}{\partial z}\right]u_z + \left[e_{33}\frac{\partial^2}{\partial r^2} + \frac{e_{33}-e_{31}}{r}\frac{\partial}{\partial r} + \frac{e_{15}}{r^2}\frac{\partial^2}{\partial\theta^2} + e_{24}\frac{\partial^2}{\partial z^2}\right]\psi = \rho\frac{\partial^2 u_r}{\partial t^2} \\
&\left[\frac{c_{66}+c_{12}}{r}\frac{\partial^2}{\partial r\partial\theta} + \frac{c_{22}+c_{66}}{r^2}\frac{\partial}{\partial\theta}\right]u_r + \left[c_{66}\frac{\partial^2}{\partial r^2} + \frac{c_{66}}{r}\frac{\partial}{\partial r} - \left(\frac{c_{66}}{r^2} - \frac{c_{22}}{r^2}\frac{\partial^2}{\partial\theta^2} - c_{44}\frac{\partial^2}{\partial z^2}\right)\right]u_\theta \\
&+\left[\frac{c_{23}+c_{44}}{r}\frac{\partial^2}{\partial z\partial\theta}\right]u_z + \left[\frac{e_{15}+e_{31}}{r}\frac{\partial^2}{\partial r\partial\theta} + \frac{e_{15}}{r^2}\frac{\partial}{\partial\theta}\right]\psi = \rho\frac{\partial^2 u_\theta}{\partial t^2} \\
&\left[(c_{55}+c_{13})\frac{\partial^2}{\partial r\partial z} + \frac{c_{23}+c_{55}}{r}\frac{\partial}{\partial z}\right]u_r + \left[\frac{c_{44}+c_{23}}{r}\frac{\partial^2}{\partial z\partial\theta}\right]u_\theta \\
&+\left[c_{55}\frac{\partial^2}{\partial r^2} + \frac{c_{55}}{r}\frac{\partial}{\partial r} + \frac{c_{44}}{r^2}\frac{\partial^2}{\partial\theta^2} + c_{33}\frac{\partial^2}{\partial z^2}\right]u_z + \left[(e_{24}+e_{32})\frac{\partial^2}{\partial r\partial z} + \frac{e_{24}}{r}\frac{\partial}{\partial z}\right]\psi = \rho\frac{\partial^2 u_z}{\partial t^2}
\end{aligned} \tag{Eq. 6-a}$$

$$\left[e_{33}\frac{\partial^2}{\partial r^2}+\frac{e_{31}+e_{33}}{r}\frac{\partial}{\partial r}+\frac{e_{15}}{r^2}\frac{\partial^2}{\partial\theta^2}+e_{24}\frac{\partial^2}{\partial z^2}\right]u_r+\left[\frac{e_{31}+e_{15}}{r}\frac{\partial^2}{\partial r\partial\theta}-\frac{e_{15}}{r^2}\frac{\partial}{\partial\theta}\right]u_\theta+$$
$$\left[\left(e_{32}+e_{24}\right)\frac{\partial^2}{\partial r\partial z}+\frac{e_{32}}{r}\frac{\partial}{\partial z}\right]u_z-\left[\eta_{33}\frac{\partial^2}{\partial r^2}+\frac{\eta_{33}}{r}\frac{\partial}{\partial r}+\frac{\eta_{11}}{r^2}\frac{\partial^2}{\partial\theta^2}+\eta_{22}\frac{\partial^2}{\partial z^2}\right]\psi=0 \qquad \text{(Eq. 6-b)}$$

The simply supported boundary conditions are (The span is θ_m)

$$u_r=\sigma_\theta=\tau_{z\theta}=\psi=0 \qquad \text{at} \quad \theta=0,\theta_m \qquad \text{(Eq. 7-a)}$$

$$u_r=\sigma_\theta=\tau_{z\theta}=\psi=0 \qquad \text{at} \quad z=0,L \qquad \text{(Eq. 7-b)}$$

The interface conditions (equilibrium and compatibility) that must be met at interfaces of all adjacent layers are expressed as (Chen 1997)

$$\sigma_r)_k=\sigma_r)_{k+1} \quad \tau_{r\theta})_k=\tau_{r\theta})_{k+1} \quad \tau_{rz})_k=\tau_{rz})_{k+1} \qquad \text{(Eq. 8-a)}$$

$$u_r)_k=u_r)_{k+1} \quad u_\theta)_k=u_\theta)_{k+1} \quad u_z)_k=u_z)_{k+1} \quad \psi)_k=\psi)_{k+1} \qquad \text{(Eq. 8-b)}$$

where k and k+1 represent typical adjacent layers. The boundary conditions of the inner and outer surfaces are

$$\sigma_r=\tau_{rz}=\tau_{r\theta}=\psi=0 \qquad \text{at} \quad r=R_i \qquad \text{(Eq. 9-a)}$$

$$\sigma_r=P_0(\theta,t), \quad \tau_{r\theta}=\tau_{rz}=0, \quad D_r=0 \qquad \text{at} \quad r=R_o \qquad \text{(Eq. 9-b)}$$

3. SOLUTION OF GOVERNING DIFFERENTIAL EQUATIONS

The solution satisfying the boundary conditions (7) may be assumed as

$$u_r=\sum_{m=1}^{\infty}\sum_{n=1}^{\infty}\phi_r(r)\sin(b_m\theta)\sin(b_n z) \qquad u_\theta=\sum_{m=1}^{\infty}\sum_{n=1}^{\infty}\phi_\theta(r)\cos(b_m\theta)\sin(b_n z)$$

$$u_z=\sum_{m=1}^{\infty}\sum_{n=1}^{\infty}\phi_z(r)\sin(b_m\theta)\cos(b_n z) \qquad \psi=\sum_{m=1}^{\infty}\sum_{n=1}^{\infty}\psi(r)\sin(b_m\theta)\sin(b_n z) \qquad \text{(Eq. 10)}$$

where: $b_m=\frac{m\pi}{\theta_m}$, $b_n=\frac{n\pi}{L}$

Substituting Eqs. (10) into the governing equations of equilibrium in terms of displacements, the partial differential equations reduce to the following ordinary differential equations.

$$\left[c_{11}\frac{d^2}{dr^2}+\frac{c_{11}}{r}\frac{d}{dr}-\left(\frac{c_{22}}{r^2}+\frac{c_{66}}{r^2}b_m{}^2+c_{55}b_n{}^2\right)\right]\phi_r+\left[-b_m\frac{c_{12}+c_{66}}{r}\frac{d}{dr}+b_m\frac{c_{22}+c_{66}}{r^2}\right]\phi_\theta$$
$$+\left[-b_n\left(c_{13}+c_{55}\right)\frac{d}{dr}+b_n\frac{c_{23}-c_{13}}{r}\right]\phi_z+\left[e_{33}\frac{d^2}{dr^2}+\frac{e_{33}-e_{31}}{r}\frac{d}{dr}-\left(\frac{e_{15}}{r^2}b_m{}^2+e_{24}b_n{}^2\right)\right]\psi=\rho\frac{\partial^2 u_r}{\partial t^2}$$

$$\left[b_m \frac{c_{66}+c_{12}}{r}\frac{d}{dr} + \frac{c_{22}+c_{66}}{r^2} b_m \right]\phi_r + \left[c_{66}\frac{d^2}{dr^2} + \frac{c_{66}}{r}\frac{d}{dr} - \left(\frac{c_{66}}{r^2} + \frac{c_{22}}{r^2} b_m{}^2 + c_{44} b_n{}^2 \right) \right]\phi_\theta$$
$$+ \left[-\frac{c_{23}+c_{44}}{r} b_n b_m \right]\phi_z + \left[\frac{e_{15}+e_{31}}{r} b_m \frac{d}{dr} + \frac{e_{15}}{r^2} b_m \right]\psi = \rho \frac{\partial^2 u_\theta}{\partial t^2}$$

$$\left[(c_{55}+c_{13}) b_n \frac{d}{dr} + \frac{c_{23}+c_{55}}{r} b_n \right]\phi_r + \left[-\frac{c_{44}+c_{23}}{r} b_n b_m \right]\phi_\theta + \left[c_{55}\frac{d^2}{dr^2} + \frac{c_{55}}{r}\frac{d}{dr} - \left(\frac{c_{44}}{r^2} b_m{}^2 + c_{33} b_n{}^2 \right) \right]\phi_z + \left[(e_{24}+e_{32}) b_n \frac{d}{dr} + \frac{e_{24}}{r} b_n \right]\psi = \rho \frac{\partial^2 u_z}{\partial t^2} \quad \text{(Eq. 11-a)}$$

$$\left[e_{33}\frac{d^2}{dr^2} + \frac{e_{31}+e_{33}}{r}\frac{d}{dr} - \left(\frac{e_{15}}{r^2} b_m{}^2 + e_{24} b_n{}^2 \right) \right]\phi_r + \left[-\frac{e_{31}+e_{15}}{r} b_m \frac{d}{dr} + \frac{e_{15}}{r^2} b_m \right]\phi_\theta$$
$$+ \left[-(e_{32}+e_{24}) b_n \frac{d}{dr} - \frac{e_{32}}{r} b_n \right]\phi_z - \left[\eta_{33}\frac{d^2}{dr^2} + \frac{\eta_{33}}{r}\frac{d}{dr} - \left(\frac{\eta_{11}}{r^2} b_m{}^2 + \eta_{22} b_n{}^2 \right) \right]\psi = 0 \quad \text{(Eq. 11-b)}$$

This system of equations are solved by considering linear shape functions N_i and N_j for $\phi_r, \phi_\theta, \phi_z$ and ψ.

$$\phi_s = \begin{bmatrix} N_i & N_j \end{bmatrix} \begin{bmatrix} \phi_{si} \\ \phi_{sj} \end{bmatrix} \quad \text{s= r, θ, z} \qquad \psi = \begin{bmatrix} N_i & N_j \end{bmatrix} \begin{bmatrix} \psi_i \\ \psi_j \end{bmatrix} \quad \text{(Eq. 12)}$$

and then applying the formal Galerkin finite element method to the first governing (o. d. e.) yields

$$\int_{r_i}^{r_j} \left\{ \begin{array}{l} \left[c_{11}\frac{d^2}{dr^2} + \frac{c_{11}}{r}\frac{d}{dr} - \left(\frac{c_{22}}{r^2} + \frac{c_{66}}{r^2} b_m{}^2 + c_{55} b_n{}^2 \right) \right]\phi_r + \left[-b_m \frac{c_{12}+c_{66}}{r}\frac{d}{dr} + b_m \frac{c_{22}+c_{66}}{r^2} \right]\phi_\theta + \\ \left[-b_n (c_{13}+c_{55}) \frac{d}{dr} + b_n \frac{c_{23}-c_{13}}{r} \right]\phi_z + \left[e_{33}\frac{d^2}{dr^2} + \frac{e_{33}-e_{31}}{r}\frac{d}{dr} - \left(\frac{e_{15}}{r^2} b_m{}^2 + e_{24} b_n{}^2 \right) \right]\psi \end{array} \right\} N_i dr = 0 \quad \text{(Eq. 13)}$$

By integrating the other ordinary differential equations, two similar to the equation (13) are obtained. Changing N_i to N_j and then repeating the above procedure, three other equations are obtained. The result is written in the following finite element equilibrium equation for each non-boundary elements:

$$[M]_e \{\ddot{X}\}_e + [K]_e \{X\}_e = \{F\}_e \quad \text{(Eq. 14)}$$

where $[M]_{8\times8}, [K]_{8\times8}$ and $\{F\}_{8\times1}$ are the mass, stiffness and force matrix respectively and

$$\{X\}_e^T = \{\phi_{ri} \quad \phi_{\theta i} \quad \phi_{zi} \quad \psi_i \quad \phi_{rj} \quad \phi_{\theta j} \quad \phi_{zj} \quad \psi_j\}$$

Deriving equilibrium condition (8) in term of displacement by using eqs. (3-5), the displacement components on the inner boundaries are obtained in term of values at neighboring nodes. Substituting results into (14) the finite element equilibrium equations for two neighboring elements at interior (k)th. and (k+1)th. interfaces are obtained as

$$[M]_k \{\ddot{X}\}_k + [K]_k \{X\}_k = \{0\} \quad , \quad [M]_{k+1} \{\ddot{X}\}_{k+1} + [K]_{k+1} \{X\}_{k+1} = \{0\} \qquad \text{(Eq. 15)}$$

Applying the boundary conditions (9) for the first and last nodes in the inner and outer surfaces and using Eqs.(14), the finite element equilibrium equations for the first and last elements become

$$[M]_1 \{\ddot{X}\}_1 + [K]_1 \{X\}_1 = \{F\}_1 \quad , \quad [M]_{MI} \{\ddot{X}\}_{MI} + [K]_{MI} \{X\}_{MI} = \{F\}_{MI} \qquad \text{(Eq. 16)}$$

Assembling Eqs. (14), (15) and (16), the general finite element equilibrium equation is obtained as

$$[M]\{\ddot{X}\} + [K]\{X\} = \{F\} \qquad \text{(Eq. 17)}$$

After establishing the finite element dynamic equation and using the Newmark method as follows

$$X(t+\Delta t) = X(t) + \Delta t \dot{X}(t) + \Delta t^2 \left\{(2-\beta)\ddot{X}(t) + \beta \ddot{X}(t+1)\right\}$$

$$\dot{X}(t+\Delta t) = \dot{X}(t) + \Delta t \left\{(1-\gamma)\ddot{X}(t) + \gamma \ddot{X}(t+1)\right\} \qquad \text{(Eq. 18)}$$

static finite element matrix equations are obtained, and then, by using the Gauss-Sidel elimination method with a suitable time step, Δt, the equilibrium equation is solved.

4. NUMERICAL RESULTS AND DISCUSSION

A sensor consisting of a three-layered cross-ply panel which its sequence lay-up is (0/90/P) composed of graphite-epoxy and piezoelectric is considered. The material properties of orthotropic piezoelectric lamina are

$$C = \begin{bmatrix} 11.5 & 7.43 & 7.78 & 0 & 0 & 0 \\ 7.43 & 13.9 & 7.43 & 0 & 0 & 0 \\ 7.78 & 7.43 & 13.9 & 0 & 0 & 0 \\ 0 & 0 & 0 & 3.06 & 0 & 0 \\ 0 & 0 & 0 & 0 & 2.56 & 0 \\ 0 & 0 & 0 & 0 & 0 & 2.56 \end{bmatrix} \times 10^{10}\,\text{Pa} \quad e = \begin{bmatrix} 15.1 & -5.20 & -5.20 & 0 & 0 & 0 \\ 0 & 0 & 0 & 0 & 0 & 12.7 \\ 0 & 0 & 0 & 0 & 12.7 & 0 \end{bmatrix} C.m^{-2}$$

$$\eta = \begin{bmatrix} 5.62 & 0 & 0 \\ 0 & 6.46 & 0 \\ 0 & 0 & 6.46 \end{bmatrix} \times 10^{-9} \quad F.m^{-1}$$

The material properties of the graphite-epoxy composite are

$$E_L = 25E_T, \quad E_T = 6.85 \text{ GPa}, \quad G_{LT} = 0.5E_T, \quad G_{TT} = 0.2E_T, \quad \nu_{LT} = \nu_{TT} = 0.25$$

where subscripts "L" and "T" denote the fiber and transverse directions, respectively. The forcing function is chosen as

$$P_0(\theta, t) = \sum_{m=1}^{\infty} P_0 (1 - e^{-\alpha t}) \sin(b_m \theta) \qquad \text{where} \quad \alpha = 13100$$

The numerical results are described in the form of maximum non dimensional displacements and stresses as follow

$$(\bar{u}_r,\bar{u}_\theta,\bar{u}_z)=\frac{100E_T}{HS^4}(u_r,u_\theta,u_z),\qquad \bar{r}=\frac{r-R_m}{H},\qquad S=\frac{R_m}{H},$$

$$(\bar{\sigma}_r,\bar{\sigma}_\theta,\bar{\sigma}_z,\bar{\tau}_{r\theta},\bar{\tau}_{rz},\bar{\tau}_{r\theta})=(\sigma_r,\sigma_\theta,\sigma_z,\tau_{r\theta},\tau_{rz},\tau_{r\theta})/P_0$$

where H is the thickness of panel.

$$R_m=1,\qquad \theta_m=\pi/3 \text{ rad.},\qquad P_0=1 \text{ Pa},\qquad S=4,\ 10,\ 20$$

Only the direct effect of piezoelectric is considered (the piezoelectric layer is served as a sensor). All curves are presented at time t=0.00675 second.

Figures 1-3 illustrate the normal stress distributions across the thickness with S. The boundary and inter laminar conditions are satisfied in them. The stresses depend strongly on the radial coordinate.

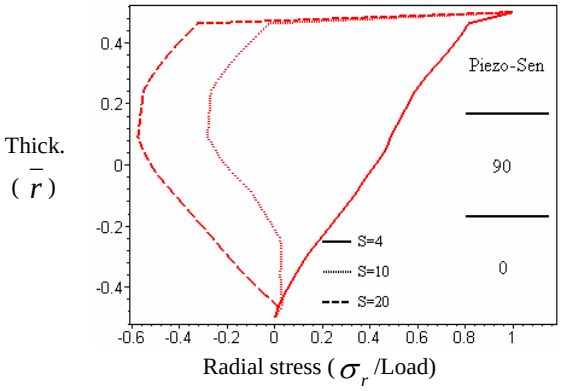

Fig. 1. Distribution of $\bar{\sigma}_r$ across the $\bar{r}$ (0/90/P,Z=L/2, $\theta=\theta_m/2$)

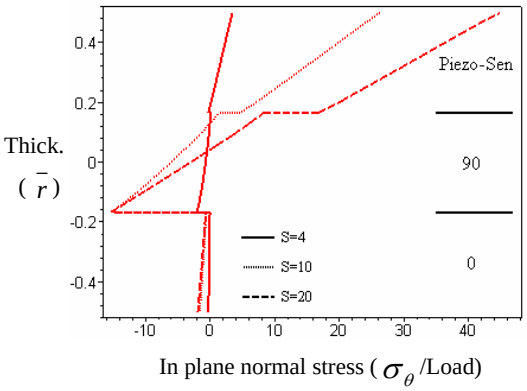

Fig. 2. Distribution of $\bar{\sigma}_\theta$ across the $\bar{r}$ (0/90/P,Z=L/2, $\theta=\theta_m/2$)

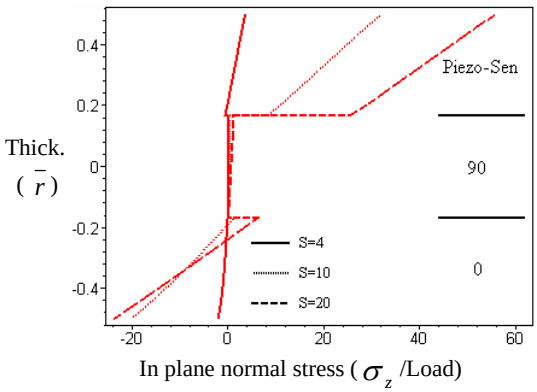

Fig. 3. Distribution of $\bar{\sigma}_z$ across the $\bar{r}$ (0/90/P,Z=L/2, $\theta=\theta_m/2$)

Figures 4 and 5 show the through-thickness distribution of transverse shear stresses, $\bar{\tau}_{r\theta}$ and $\bar{\tau}_{rz}$. The boundary and inter laminar equilibrium conditions are satisfied. These figures have a near-parabola form for each layer.

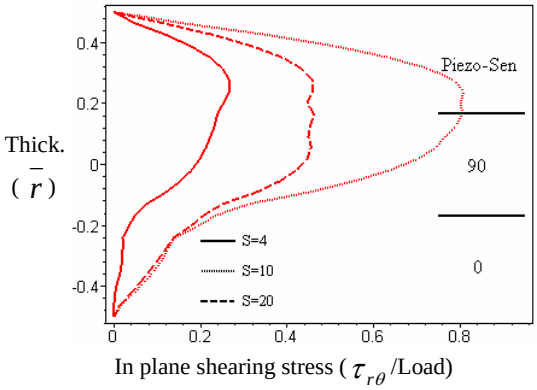

Fig. 4. Distribution of $\bar{\tau}_{r\theta}$ across the $\bar{r}$ (0/90/P,Z=L/2, $\theta = 0$)

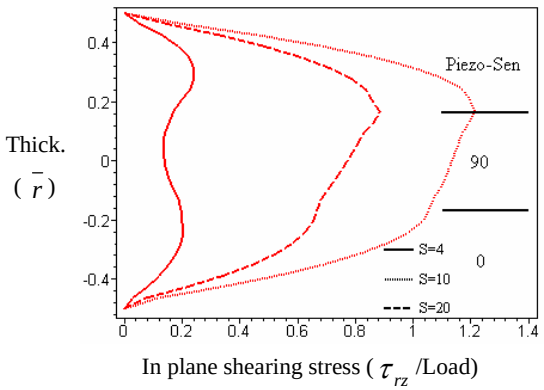

Fig. 5. Distribution of $\bar{\tau}_{rz}$ across the $\bar{r}$ (0/90/P,Z=0, $\theta = \theta_m / 2$)

In Figures 6-8, the distributions of the mechanical displacements in the radial direction due to different S are presented. The boundary and inter laminar equilibrium conditions are satisfied. In these figures the slopes imply in-plane strains that are discontinuous in the interfaces.

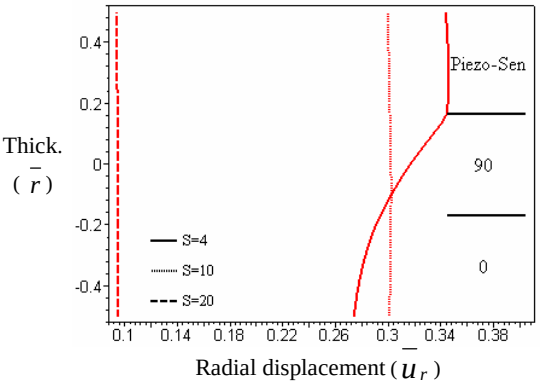

Fig. 6. Distribution of $\bar{u}_r$ across the $\bar{r}$ (0/90/P,Z=L/2, $\theta = \theta_m / 2$)

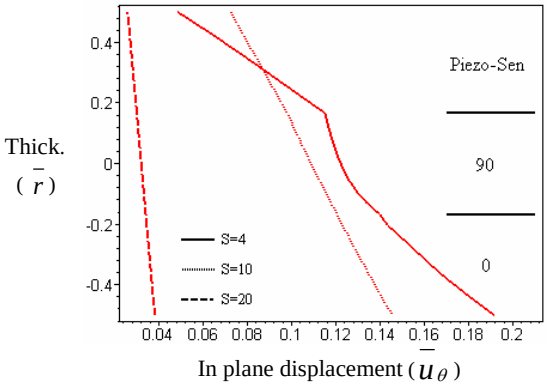

Fig. 7. Distribution of $\bar{u}_\theta$ across the $\bar{r}$ (0/90/P,Z=L/2, $\theta = 0$)

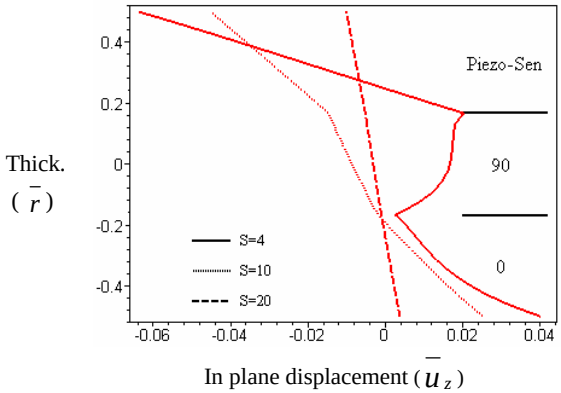

Fig. 8. Distribution of $\bar{u}_z$ across the $\bar{r}$ (0/90/P,Z=0, $\theta = 0$)

Figure 9 shows the electric potential distribution corresponding to different S. The distribution of the electric potential depends on S. When S is more than 4, the electric potential in the sensor will change linearly. This is different from the results of Kapuria (1997).

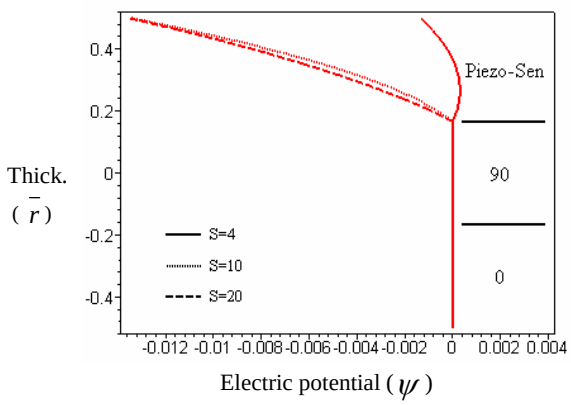

Fig. 9. Distribution of $\bar{\psi}$ across the $\bar{r}$ (0/90/P,Z=L/2, $\theta = \theta_m / 2$)

Figures 10-13 show the effect of boundary conditions on the distributions of the mechanical displacements, mechanical stresses and electric potential in the axial direction. In these figures the behavior of piezoelectric laminate are similar to multi-layered composite panel.

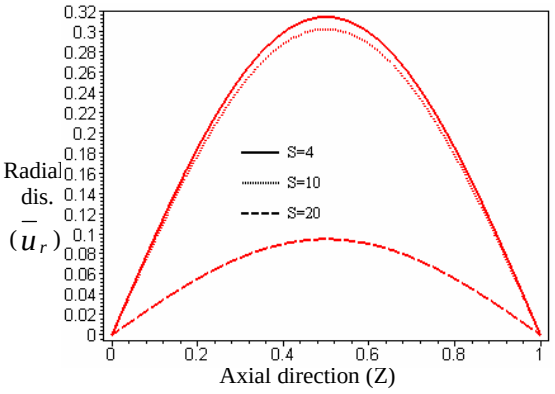

Fig. 10. Distribution of $\bar{u}_r$ across the Axial Direction (0/90/P, $r = R_m$, $\theta = \theta_m / 2$)

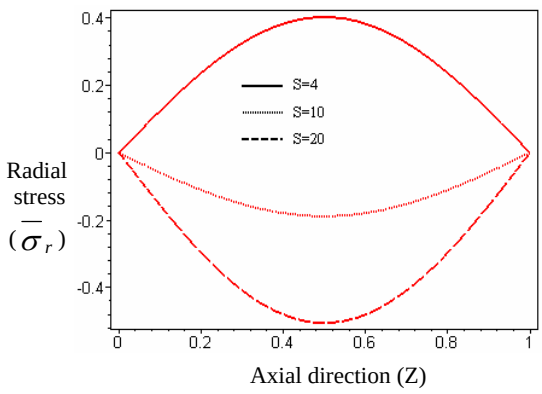

Fig. 11. Distribution of $\bar{\sigma}_r$ across the Axial direction (0/90/P, $r = R_m$, $\theta = \theta_m / 2$)

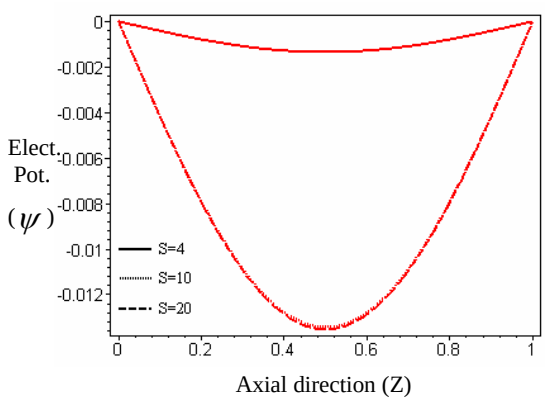

Fig. 12. Distribution of ψ across the Axial direction (0/90/P, $r = R_a, \theta = \theta_m / 2$)

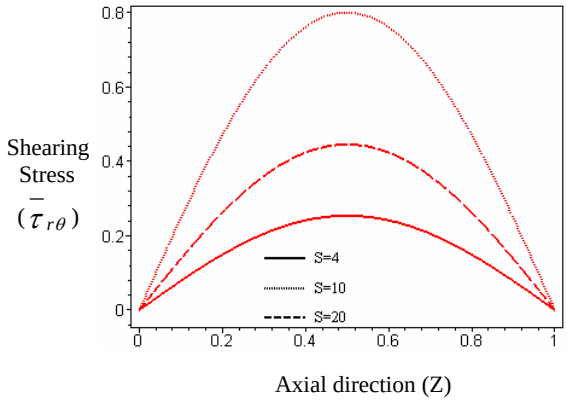

Fig. 13. Distribution of $\bar{\tau}_{r\theta}$ across the Axial direction (0/90/P, $r = R_m, \theta = 0$)

The time histories of the radial and circumferential displacement, $\bar{u}_r, \bar{u}_\theta$ in middle layer of panel, are shown in Fig. 14 and 15 respectively. The variations in amplitude and period of motion in radial direction are similar to those for the circumferential direction.

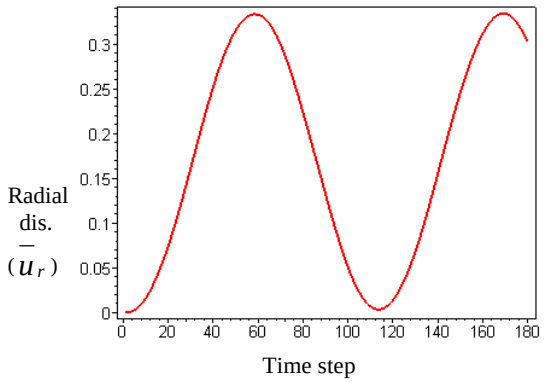

Fig. 14. Variation in $\bar{u}_r$ with time (0/90/P,S=20,Z=L/2, $\theta = \theta_m / 2$)

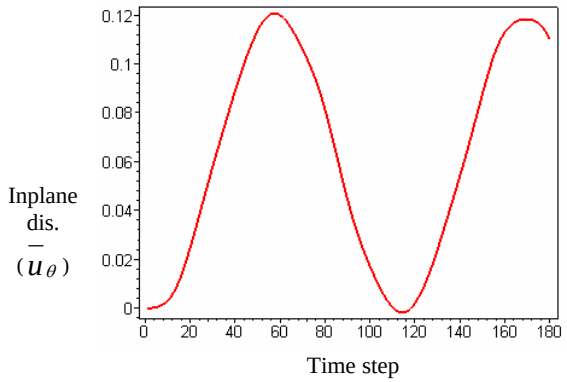

Fig. 15. Variation in $\bar{u}_\theta$ with time (0/90/P,S=20,Z=L/2, $\theta = 0$)

The time histories of the electric potential, ψ, in outer surface, is also shown in Fig. 16. In this figure the period of motion is similar to thus for the mechanical displacements.

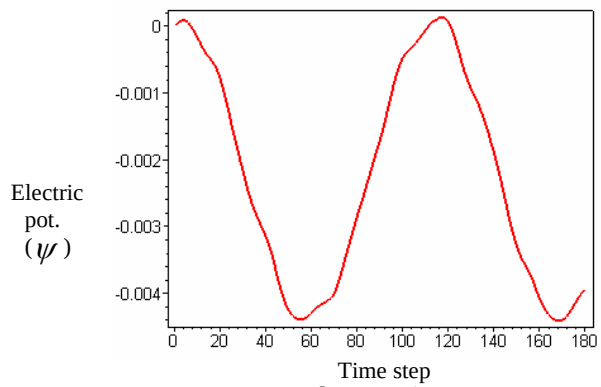

Fig. 16. Variation in ψ with time (0/90/P,S=20,Z=L/2, $\theta = \theta_m / 2$)

From the above studies, we can conclude that the linear variation assumption of the electric potential in the piezoelectric layer must be treated with caution and the three-dimensional methods for the piezoelastic response analysis are shown to be the preferred ones.

5. CONCLUSION

A study on the three-dimensional elasticity solution of shell panel piezoelectric sensor is presented. In this paper, the structure is finitely long, simply-supported, orthotropic and under pressure excitation. The present study has shown that the Fourier series expansion method is suitable for the mechanical displacement and electric potential analysis in panel-type sensors.

The direct piezoelectric effect of the piezoelectric layer subjected to outer pressure is investigated in detail. It is always assumed in the analytical analysis of the piezoelectric structures that the electric potential in the piezoelectric layers varies linearly and the displacements change in the form of prescribed functions across its thickness (Kapuria 1997). However, it has been shown that the distributions of the mechanical displacements and electric potential of piezoelectric response are very complicated and cannot be treated as pure elastic structures or piezoelectric structures. Therefore, three-dimensional analysis of piezoelastic behavior of structures is recommended even for thin laminated structures. Since a comprehensive and exact study of active piezoelectric structures is still unavailable, the present work provides an enhanced insight to the mechanical and electric behaviors of this type of smart structure. Results presented in this paper are also useful for assessing approximate analysis.

REFERENCES

Alibiglu A., Shakeri M. and Eslami M.R. (2002), Elasticity solution for thick laminated anisotropic cylindrical panels under dynamic load, J. Mech. Eng. Sci. Vol. 216 Part C, I Mech E.

Chen C-Q, Shen Y-P, and Wang X-M (1996), Exact solution for orthotropic cylindrical shell with piezoelectric layers under cylindrical bending, Int. J. Solids Struct., Vol. 33(30), pp. 4481-4494.

Daneshmehr A., Shakeri M., (2004), Analysis of thick laminated panel with piezoelectric sensors based on three-dimensional theory of elasticity, ICTAM04 Conf., Warsaw, Poland.

Daneshmehr A., Shakeri M. (2004), The response analysis of the piezoelectric shell panel actuators based on the theory of elasticity, ESDA04 Conf. (ASME), Manchester, United Kingdom.

Dumir P.C., Dube G.P., and Kapuria S. (1997), Exact piezoelastic solution of simply-supported orthotropic circular cylindrical panel in cylindrical bending, Int. J. Solids Struct., Vol. 34(6), pp. 685-702.

Kapuria S., Sengupta S., and Dumir P.C. (1997), Three-dimensional solution for simply-supported piezoelectric cylindrical shell for axisymmetric load, Compu. Methods in Appl. Mech. Eng., Vol. 140(1-2), pp. 139-155.

Shakeri M., Daneshmehr A. and Alibiglu A., (2003), Elasticity solution of thick laminated cylindrical panel with piezoelectric layer under cylindrical bending, EASEC-9 Conf., Bali, Indonesia.

Shakeri M., Daneshmehr A., (2004), Three dimensional elasticity solution for finite thick laminated shell panel with piezoelectric layers, J. Mech. En., Iran.

Tzou H.S., and Gadra M., (1989), Theoretical analysis of a multilayered thin shell coupled with piezoelectric shell actuators for distributed vibration controls, J. Sound Vibration, Vol. 132, pp. 433-450.

Tzou H.S., (1992), A new distributed sensors and actuator theory for intelligent shells, J. Sound Vibration, Vol. 153, pp. 335-349.

Tzou H.S., and Tseng C.L., (1991), Distributed modal identification and vibration control of continua: piezoelectric element formulation and analysis, ASME J. of Dynamic Sys., Measurement and Con., Vol. 113, pp. 500-505.

Tzou H.S., and Ye R., (1994), Piezothermoelasticity and precision control of piezoelectric systems, ASME J. of Vib. and Acoustics, Vol. 116, pp. 489-495.

Tzou H.S. and Zhong J.P. (1993), Electro mechanics and vibrations of piezoelectric shell distributed systems. J Dyn Syst. Meas Control, Vol. 115(3), pp. 506-517.

Tzou H.S. and Zhong J.P. (1994), Linear theory of piezoelectric shell vibrations, J. Sound Vib., Vol. 175(1), 77-88.

